Rev. ANL/HEP 7339

The Double-Pomeron Exchange Contribution to the Reaction $pp \rightarrow pp\pi^+\pi^-$ at 205 GeV/c*

M. DERRICK, B. MUSGRAVE, P. SCHREINER and H. YUTA

Argonne National Laboratory, Argonne, Illinois 60439

The reaction $pp \rightarrow pp\pi^+\pi^-$ at 205 GeV/c is analyzed in terms of the rapidities of the secondary particles to measure the contribution of the double-Pomeron exchange process. Using a sample of 191 events, we estimate the maximum possible contribution for this process to be 44 μb for the region of πp effective mass greater than 2.0 GeV in a total cross section of 680 ± 140 μb.

*Work supported by the U. S. Atomic Energy Commission.

The multiperipheral model has had considerable success in recent years in explaining many of the features of high energy reactions observed at the CERN Intersecting Storage Ring and with the bubble chamber at the National Accelerator Laboratory (NAL).[1] The nature of the exchanged particles has not been explicitly studied except that Pomeron exchange is thought to be responsible for the diffractively-produced events. In one of the simplest multiperipheral models,[2] multi-Pomeron exchange processes with non-zero couplings would lead to divergence problems in the cross section, so it is important to search for evidence of multi-Pomeron exchange.

We have looked for double-Pomeron exchange (DPE) in the reaction

$$pp \rightarrow p\pi^+\pi^- p \qquad (1)$$

at 205 GeV/c which would occur via the diagram of Fig. 1(a). This diagram, with a single pion loop, is perhaps the simplest case where one might see evidence for DPE. Reaction (1) has been extensively studied for momenta up to 28 GeV/c,[3] and several attempts have been made to evaluate the DPE contribution.[4, 5] However, at low energies such a contribution in the central rapidity region is essentially masked by the pronounced low $p\pi^+\pi^-$ mass enhancements resulting from diagrams such as 1(b) and 1(c), so that the earlier estimates were not conclusive. The present experiment has the advantage that at our high energy a much larger range of rapidity space is available to the secondaries, which reduces the degree of overlap between the diffractive and any DPE contributions in the central rapidity region.

The data were obtained from 50, 000 pictures taken with the 30-inch hydrogen bubble chamber exposed to a 205 GeV/c proton beam at NAL. The results reported here are based on 191 $pp\pi^+\pi^-$ events selected by kinematic fitting from 1175 successfully reconstructed four-prong events in a 36 cm long fiducial volume. A detailed discussion of the fitting and event selection is contained in Ref. 6. We measure the cross section for reaction (1) to be 680 ± 140 μb, where the error quoted includes our estimate of the possible contamination.

Fig. 2(a, b, c, d) shows the $p\pi^+\pi^-$, $p\pi^+$, $p\pi^-$, and $\pi^+\pi^-$ mass distributions, respectively, and summarizes the prominent features of the reaction (1). The low $p\pi^+\pi^-$ mass enhancement, which results from diffractive excitation of the proton, and pronounced $p\pi^+$ and $p\pi^-$ low mass peaks dominate the reaction in a way similar to what is seen at lower energies. The $\pi^+\pi^-$ mass distribution in Fig. 1(d) shows that the dipion mass tends to be small with most events falling below the ρ mass. There is no evidence for strong production of either $\rho(765)$ or f(1260), in qualitative agreement with results at 24 GeV/c. [5]

To isolate the DPE contribution, one can impose cuts on the various sub-energies to restrict the rapidities of the secondaries. Fig. 3(a, b, c) shows the longitudinal center of mass (CM) rapidity distributions of the pions and protons for the fitted events. There is good overall forward-backward symmetry in each case, demonstrating that our fitted sample is not strongly

affected by any bias or contamination. Overall, the low mass $p\pi\pi$ system is associated with a single proton in the opposite hemisphere with an average gap from this leading proton to the $p\pi\pi$ system of ~ 5 units. A rapidity correlation study of the low $p\pi^+\pi^-$ and $\pi^+\pi^-$ mass distribution indicates that most of the $\pi^+\pi^-$ pairs are emitted as a result of diffractive excitation of either the beam or the target proton. Since we expect the pion pairs from the DPE process to have a large rapidity gap from both protons, we first impose a restriction that the longitudinal CM rapidities of the π^+ and π^- lie between the two proton rapidities as shown in diagram of Fig. 1(a). Events selected in this way are shown hatched in Fig. 2.

Fig. 3(d) shows the longitudinal CM rapidity ($Y_{\pi\pi}$) distribution for the $\pi^+\pi^-$ system considered as a single particle. The hatched area again corresponds to the rapidity selection described above. The clear double-peaked structure is attributed to the $p\pi^+\pi^-$ low mass enhancement observed in Fig. 2(a). We also note that the distribution is flat in the central region where the double-Pomeron contribution is expected to contribute. This is true for both the total sample as well as for the hatched events. However, because of the tails from the diffractive process, any estimate of the DPE contribution can be strongly influenced by the parameterization adopted for the diffractive process.

To isolate a possible DPE contribution, we simply define as diffractive those events having any one of the four possible $p\pi$ masses less than 2.0 GeV. This leaves the nine events[7] shown in black on Figs. 2(a, d) and Fig. 3(d).

Most of the nine events are in the central region of rapidity, i.e., $|Y_{\pi\pi}| < 1.0$. Effectively, these mass cuts remove all the events having $p\pi^+\pi^-$ mass less than 3 GeV as well as the low mass $p\pi^+$ and $p\pi^-$ enhancements. The remainder contains the possible DPE contribution plus other contributions such as single diffraction in the region of $p\pi$ mass greater than 2 GeV, and these nine events correspond to a cross section of 44 ± 15 μb.

However, we find that the events in the central rapidity region mainly come from those with $\pi^+\pi^-$ mass greater than 0.6 GeV, whereas we expect the DPE process to be dominated by a low mass s-wave $\pi\pi$ system. This is best shown by the $Y_{\pi\pi}$ distributions of Fig. 3(e, f) where the $\pi^+\pi^-$ mass is selected to be less than 0.6 GeV and greater than 0.6 GeV, respectively. As indicated by the hatching, events in both plots satisfy the rapidity ordering previously discussed. We note that with the restriction of $M_{\pi\pi} < 0.6$ GeV, we obtain a cross section of 9 μb based on two events.

The diagrams of Fig. 1 assuming a fixed $\pi\pi$ mass suggests a $Y_{\pi\pi}$ distribution of the form[8]

$$\frac{dN}{dY_{\pi\pi}} = 2A^2 \cosh^2(\delta Y_{\pi\pi}) + 2AB \cosh(\delta Y_{\pi\pi}) + B^2 ,$$

where A and B are the parameters to characterize the diffraction and the double-Pomeron processes, respectively, and δ is the difference between the intercepts of the Pomeron and the f Regge-trajectories, taken to be 0.5. We have fitted the hatched distribution in Fig. 3(d) to this form. In the fit, we only consider $|Y_{\pi\pi}| < 2.0$ where the above formula should be

appropriate to our data. We find that the DPE parameter B is consistent with being zero.[9] The best fit curve is shown in Fig. 3(d). We note that the non-zero value in the central rapidity region comes from the diffractive component of $2A^2$.

A naive calculation of the DPE contribution based on the ABFST model,[2] without introducing any form factor, gives a cross section of 70 μb[10] for the region of the $p\pi$ mass greater than 2 GeV and $|t_{\pi\pi}| < 0.5$ GeV^2. Here $t_{\pi\pi}$ is the momentum transfer squared between the two pions as shown in diagram (a) of Fig. 1. For the same $p\pi$ mass and $t_{\pi\pi}$ selection, we measured a cross section of 24 μb which is substantially less than that calculated.

In conclusion, we see no evidence for a double-Pomeron exchange contribution to the $p\pi^+\pi^-p$ final state and measure the maximum possible DPE contribution of 44 ± 15 μb for the region of the $p\pi$ mass greater than 2 GeV. Compared to a naive ABFST calculation of the DPE contribution in a restricted $p\pi$ mass and $t_{\pi\pi}$ region, our data give a cross section which is smaller by a factor of about 3.

We acknowledge the effort of the NAL staff for providing this exposure and of the ANL film scanning group. We are also grateful to D. Sivers, D. Snider, S. Pinsky, B. Webber and R. Shankar for stimulating discussions.

References

1. M. Jacob, "Multi-Body Phenomena in Strong Interactions," TH 1683-CERN (1973).

2. G. F. Chew et al., Phys. Rev. D2, 765 (1970); L. Bertocchi et al., Nuovo Cimento 25, 626 (1962); D. Amati et al., Nuovo Cimento 26, 6 (1962).

3. "Compilation of Cross Sections I; Proton-Induced Reactions," CERN/HERA 70-2 (1970).

4. J. G. Rushbrook, "Diffraction Production Processes," Proceedings of the Third International Colloquium on Multiparticle Reactions; ed. O. Czyzewski and L. Michejda, Zakopane (1972) p. 441.

5. U. Idschok et al., Nucl. Phys. B53, 282 (1973).

6. M. Derrick et al., "The Reaction $pp \to pp\pi^+\pi^-$ at 205 GeV/c," submitted to Phys. Rev. D.

7. D. M. Chew and R. Shankar, "Further Selection of Double-Pomeron Events and Theoretical Justifications," Lawrence Berkeley Laboratory Physics Note TG-205 (1973) and to be published in Nucl. Phys. B. If we remove events having either $p_1\pi_1$ or $p_2\pi_2$ mass less than 2 GeV where p_i and π_i $(i = 1, 2)$, respectively, denote the proton and pion of Fig. 1(a), we obtain an extra two events. Both of them have a smaller $p\pi\pi$ mass than 3 GeV and a large $|Y_{\pi\pi}|$ of order of 2.

8. We thank S. Pinsky for providing the formula.

9. Without restrictions on the parameter B, we obtain a negative value of B from the fit. Since the parameter B is physically expected to be positive, the best fit is obtained by setting B = 0 and gives A = 1.89 ± 0.06.

10. We thank D. Snider for calculating the cross section.

Figure Captions

Fig. 1 Feynman diagrams representing (a) double-Pomeron exchange, (b) and (c) diffractive production of the $p\pi^+\pi^-$ system.

Fig. 2 The effective mass distribution for (a) the $p\pi^+\pi^-$, (b) the $p\pi^+$, (c) the $p\pi^-$, and (d) the $\pi^+\pi^-$ systems. The hatched events correspond to those where both protons are at the ends of the rapidity chain; the shaded events also have the $p\pi$ effective masses greater than 2 GeV.

Fig. 3 The CM longitudinal rapidity distribution for (a) the π^+, (b) the π^- and (c) the proton from reaction (1) and the CM rapidity distribution for the $\pi^+\pi^-$ system, (d) for all the $\pi\pi$ mass range, (e) for the $\pi\pi$ mass less than 0.6 GeV and (f) for the $\pi\pi$ mass greater than 0.6 GeV. The hatched events correspond to those where both protons are at the ends of the ordered rapidity chain; the shaded events also have the $p\pi$ effective masses greater than 2 GeV.

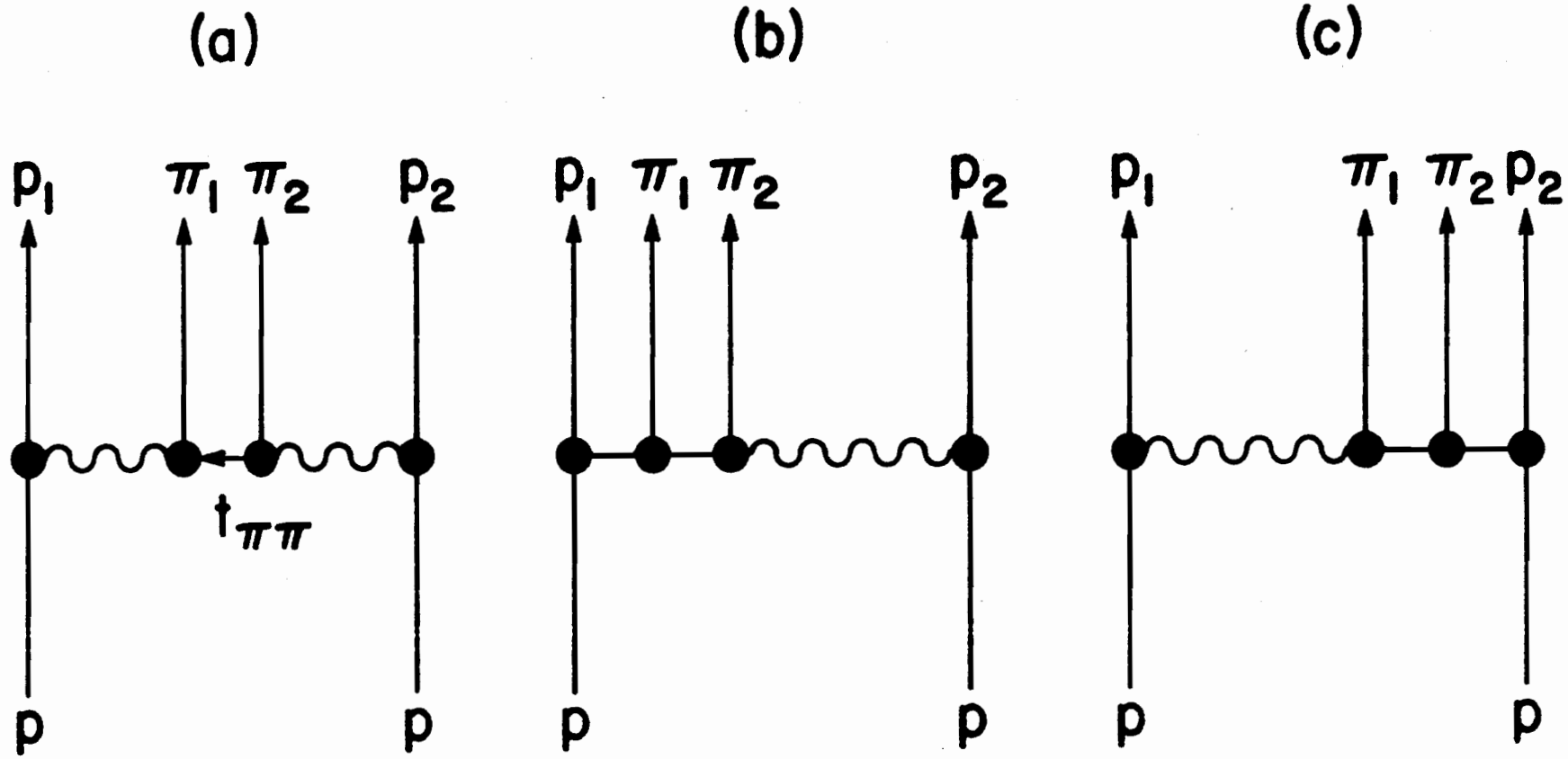

Fig. 1

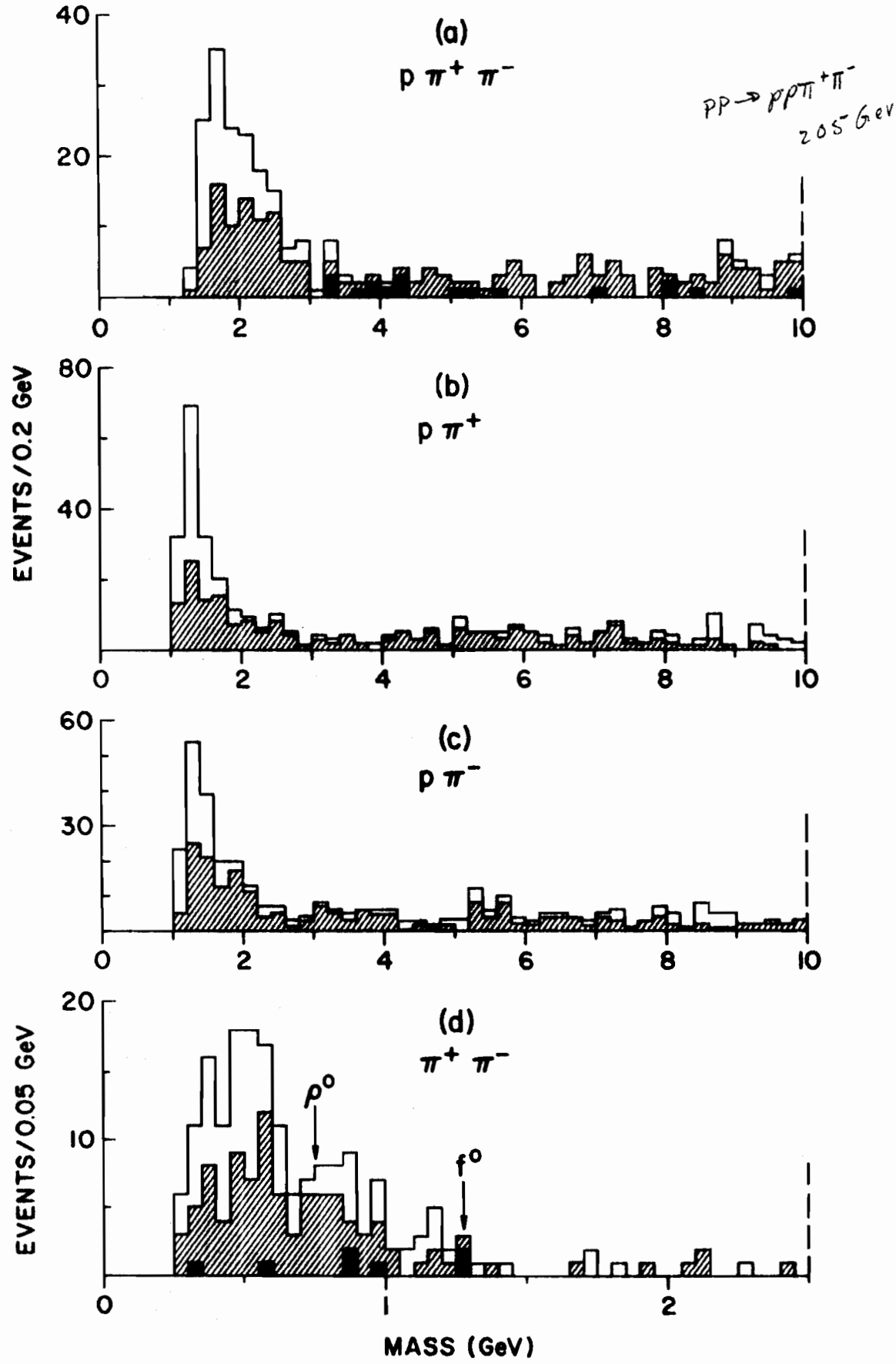
(a)
p π+ π−
pp → ppπ+π−
205 GeV
(b)
p π+
(c)
p π−
(d)
π+ π−
ρ°
f°
EVENTS/0.2 GeV
EVENTS/0.05 GeV
MASS (GeV)

Fig. 2

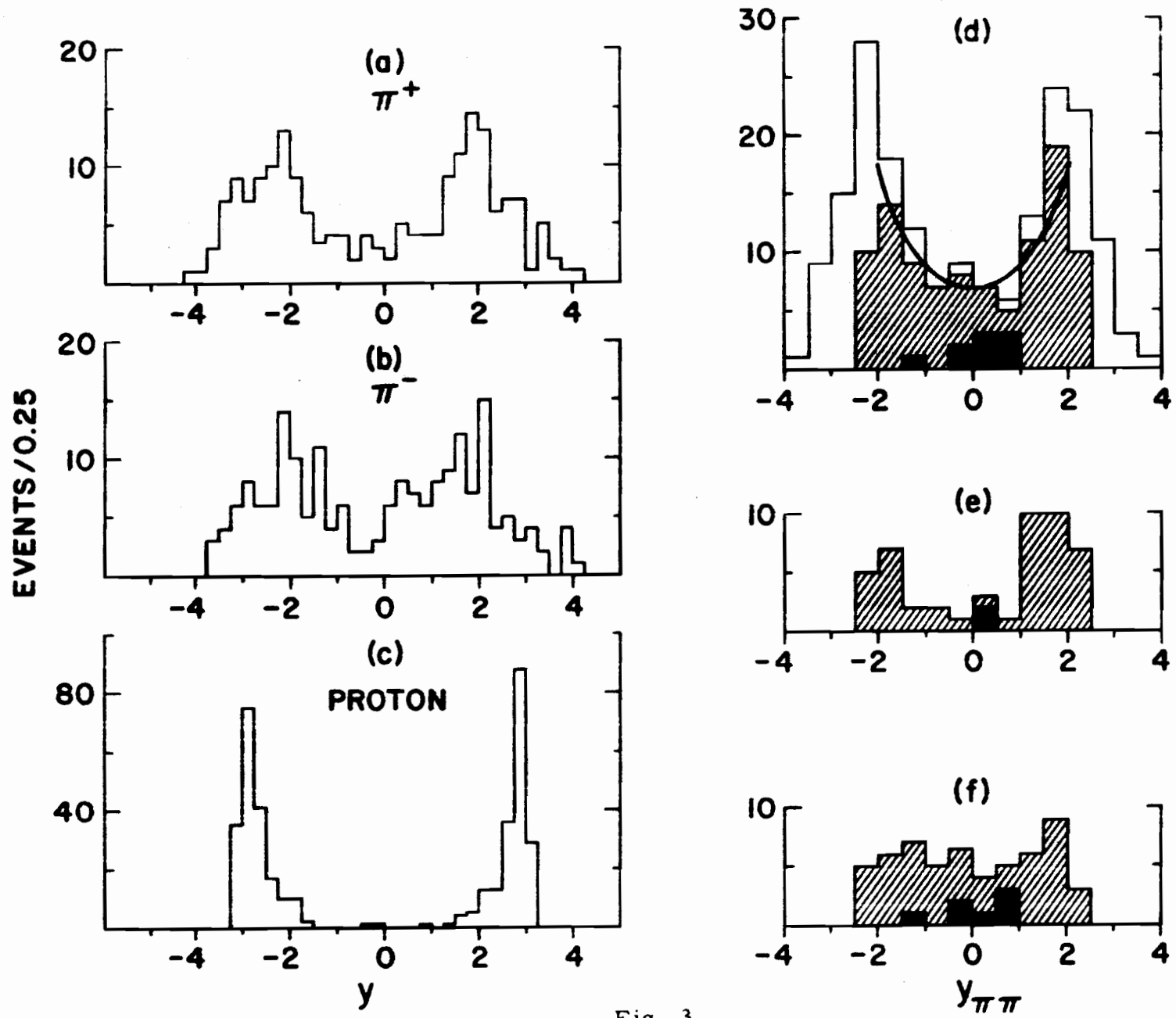

Fig. 3